13th Australasian Fluid Mechanics Conference
Monash University, Melbourne, Australia
13-18 December 1998

MEANDERING PLUME MODELS IN TURBULENT FLOWS

Michael S. BORGAS

CSIRO Atmospheric Research
Station St. Aspendale, Victoria, AUSTRALIA

ABSTRACT

A new interpretation of meandering plumes is proposed based on Lagrangian statistics of *N*-particle clusters. The key element is the Gaussian nature of the cluster 'shape' contrasting with the non-Gaussian nature of the 'size.' This process is illustrated by the dynamics of random Lagrangian triangles formed by triads of tracer particles obtained from direct numerical simulations of turbulence. The *N*-particle model leads to simple expressions for the probability density function of plume concentration in terms of classic relative dispersion of particle pairs.

INTRODUCTION

Passive scalar transport and mixing is often best considered from a Lagrangian point of view, at least when the scalar is released from isolated sources (Sawford, 1985). For atmospheric pollution, it is often a plume from a factory chimney or an accidental toxic release that must be modelled for risk assessment, which requires probabilities of concentration levels rather than simple quantities like the mean concentration. Gifford's meandering plume model (Gifford, 1959) addresses this problem by flapping a prescribed local concentration profile according to the prevailing large-scale turbulence. It captures some aspects of turbulent mixing, but does not represent in-plume concentration fluctuations. This type of meandering plume model requires a separation of scales between large-scale flapping and in-plume turbulent mixing, which is not always clearly defined. Here we consider new models for plume mixing based on multi-particle Lagrangian statistics in turbulence. The standard results (Sawford, 1985) are for statistics of single particles and pairs of particles in turbulent flows, which give the mean and variance of a scalar field at time t and position $\underline{x}$ for a source, $S(\underline{y})$, defined at time $t = t_0$, but more generally (overbar indicates an average)

$$\overline{C^N(\underline{x},t)} = \int P_N\left(\underline{x}_1,\underline{x}_2,\ldots,\underline{x}_N,t_0;\underline{x},\underline{x},\ldots,\underline{x},t\right)\times S(\underline{x}_1)S(\underline{x}_2)\ldots S(\underline{x}_N)d^3\underline{x}_1 d^3\underline{x}_2\ldots d^3\underline{x}_N, \quad (1)$$

where P_N is the transition probability density function (pdf) for N particles to have come initially from $\underline{x}_1,\ldots,\underline{x}_N$, and to have reached $\underline{x}$ (the concentration measurement point) at time *t*. These ideas have been used widely, and recently Borgas & Sawford (1996) compared Lagrangian-model predictions for fluctuations (N=1,2) with wind-tunnel (passive) temperature measurements, demonstrating the utility of the particle models. However, despite the importance of the mean and the fluctuation, it would be useful to have predictions for the probability density function of concentration, $P(C)$ (equivalent to arbitrarily many of the higher-order moments of the scalar field at the point $\underline{x}$, $\overline{C^N}$ for $N = 1,2,\ldots$).

Meandering Turbulent Plumes

Gifford's meandering-plume is illustrated in Figure 1.

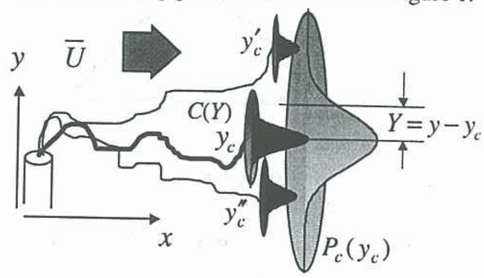

Figure 1 : Schematic of a meandering plume.

A fixed instantaneous in-plume concentration profile $C(Y)$, where Y measures distance from the instantaneous centre-of-mass y_c, is randomly flapped about according to the energy-containing scales of the turbulence. The statistics of the 'flap' of y_c, written as $P_c(y_c)$, are also assumed known. y_c' and y_c'' are simply two other independent 'flap' realisations. The concept relies on separation of turbulent scales: large eddies flapping the plume and small eddies locally mixing the plume. It therefore has restricted foundations and relies on assumed inputs which are not straightforward. For example, the original meandering plume (Gifford, 1959) imposed a Gaussian in-plume (instantaneous) profile and a Gaussian distribution for the random centre-of-mass displacements. Model variants have included top-hat distributions for $C(Y)$, to better account for plume structure, and even prescribed distributions for fluctuating $C(Y)$, but only ever with an empirical justification. Here we avoid much arbitrariness and are able to deal with a continuous spectrum of turbulent scales without partitioning the plume dynamics into meandering motions and in-plume scales. By including in a single framework the energy containing bulk displacements and the ubiquitous cascading fine-scale motions, say parameterised by turbulent energy dissipation rate, $\overline{\varepsilon}$, which controls the rate of small-scale mixing, better founded modelling is possible.

MULTI-PARTICLE LAGRANGIAN STATISTICS

The specific new results here are for triads of particles, evolving as Lagrangian variables, which explicitly determine the skewness of the scalar field. The essential physics is simply captured by considering the joint behaviour of three inter-particle spacings, r_1, r_2 and r_3. Taken individually, each spacing is just a two-particle separation statistic, for example, $\langle r_1 \rangle = \langle r_2 \rangle = \langle r_3 \rangle = \langle r \rangle$ (the average separation). However, taken together the spacings define a random triangle, whose Lagrangian size and shape characterise the three-particle cluster.

Random Lagrangian Triangles

Figure 2 shows a triangle where the three vertices are interpreted as separate Lagrangian particles advected by a turbulent flow. The random triangle shape reflects the role of turbulent flow structures encountered in flight.

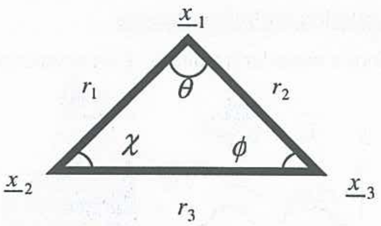

Figure 2 : Random triangle notation. Initial vertices are coincident, each then has equivalent statistics.

The mean-square behaviour of any of the sides is just

$$\langle \underline{r}_1 \cdot \underline{r}_1 \rangle = 2\langle \underline{x}_1 \cdot \underline{x}_1 \rangle - 2\langle \underline{x}_1 \cdot \underline{x}_2 \rangle = \sigma_r^2 ,$$

(the relative dispersion) while for pairs of sides,

$$\begin{aligned} \langle \underline{r}_1 \cdot \underline{r}_2 \rangle &= \langle \underline{x}_1 \cdot \underline{x}_2 \rangle + \langle \underline{x}_3 \cdot \underline{x}_2 \rangle - \langle \underline{x}_2 \cdot \underline{x}_2 \rangle - \langle \underline{x}_1 \cdot \underline{x}_3 \rangle \\ &= \langle \underline{x}_1 \cdot \underline{x}_2 \rangle - \langle \underline{x}_1 \cdot \underline{x}_1 \rangle = -\tfrac{1}{2}\langle \underline{r}_1 \cdot \underline{r}_1 \rangle . \end{aligned} \qquad (2)$$

The geometric identity (2) forces the correlation coefficient for any two sides of the triangle to be exactly minus one half. This greatly facilitates modelling. For example, assuming Gaussian triangle statistics leads to the probability density for sides r_1, r_2 and angle θ:

$$p(r_1, r_2, \theta) = r_1^2 r_2^2 \left(\tfrac{4}{3}\right)^{\frac{3}{2}} \frac{\sin\theta}{\pi\sigma_r^6} \exp\left(-\frac{r_1^2 - r_1 r_2 \cos\theta + r_2^2}{\frac{3}{2}\sigma_r^2} \right).$$

A specific prediction is that the mean area of triangles in flight can be expressed as $\langle A \rangle = 1/2\langle r_1 r_2 \cos 6 \rangle = \sqrt{3}/6\sigma_r^2$. This and other properties of triangles will be tested using direct turbulence simulation data of Yeung (1994). For this purpose we also choose a second simple geometric entity which is the probability density for the maximum angle for the triangle (measured in radians):

$$\begin{aligned} \tilde{p}(\theta_{\max}) &= 3 \int_{\pi - 2\theta_{\max}}^{\theta_{\max}} \hat{p}(\theta_{\max}, \chi) d\chi & \frac{\pi}{3} \le \theta_{\max} \le \frac{\pi}{2} \\ &= 3 \int_{0}^{\pi - \theta_{\max}} \hat{p}(\theta_{\max}, \chi) d\chi & \frac{\pi}{2} \le \theta_{\max} \le \pi \end{aligned} \qquad (3)$$

where the two-angle ($\theta + \chi + \phi = \pi$) pdf $\hat{p}(\theta, \chi)$ is

$$\hat{p}(\theta, \chi) = \frac{3^{3/2} \sin^2\theta \sin^2\chi \sin^2(\theta + \chi)}{\pi\left(\sin^2\theta + \sin\theta \sin\chi \sin(\theta + \chi)\right)^3} .$$

Numerical Simulations of Turbulence

We use some results from direct numerical simulations of isotropic turbulence (Yeung, 1994), there analysed to give classic Lagrangian pair statistics. Lagrangian particle trajectories have been recently re-analysed (Yeung, 1997) to give Lagrangian triangle statistics. The results are for forced isotropic turbulence at Taylor-scale Reynolds number $\mathrm{Re}_\lambda = 140$. Here we wish to emphasise behaviour relevant for the inertial-range scales, and choose three initial separations for equilateral triangles

$$r_1 = r_2 = r_3 = 16\eta, 64\eta, 128\eta .$$

where η is Kolmogorov's microscale length; the largest separation is comparable with an integral length scale of the turbulence. Results are shown in figures 3 for the time development of the area to dispersion ratio, showing evolution from the imposed equilateral initial condition ($\langle A \rangle = \sqrt{3}/4\sigma_r^2$), to the Gaussian limit. The straining action of the turbulence shears the triangles, drawing them out into longer more slender objects, causing the area to fall relative to the dispersion, but an equilibrium ratio is soon reached. In figure 4 maximum angle statistics are shown (in degrees) at a particular time (for inertial-range separations at least for the smallest initial triangle). There is good collapse onto the analytic Gaussian results.

These results suggest that relatively simple processes are at work: the main action of relative-dispersion stretching

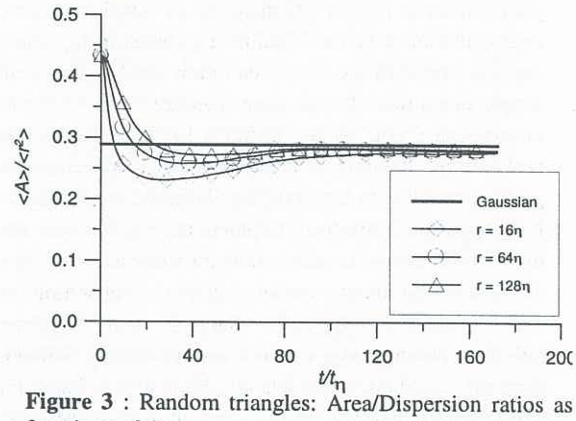

Figure 3 : Random triangles: Area/Dispersion ratios as functions of time.

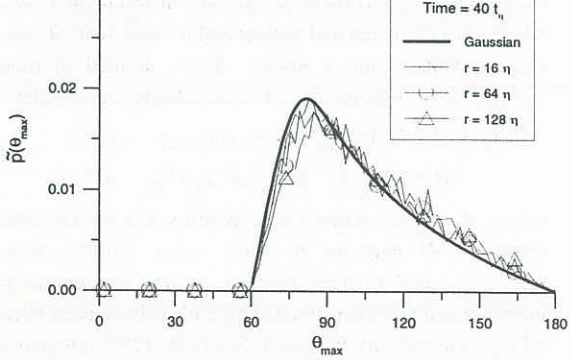

Figure 4 : Random triangles: maximum-angle statistics at a fixed time.

(increasing pair separation), and a random 'folding' of the triangle (shape distortion). The stretching is described by two-particle relative dispersion (the statistics of r), which is comparatively well known. Meanwhile the triangle shape fluctuates in time between (nearly) isosceles, through equilateral, to isosceles again, but generally with a different smallest side in successive cycles. Equivalently, the angles between the sides, cycle randomly between $0°$ and $180°$. The triangle shapes are almost purely random with approximately 'Gaussian' statistics (figures 3 & 4). This means that the shape of the triangle decouples from the size of the triangle, and, whereas the size is determined by the dynamics of turbulence (essentially the energy dissipation rate), the shape is determined simply by topological factors. For example, simple formulas for probability distributions of triangle angles and side-ratios can be given which are universal with no physical parameters (initial transients can be reduced by using initial Gaussian random triangles rather than specific equilateral triangles).

CONCENTRATION PROBABILITY DENSITIES

The simplicity of the three particle results suggests immediate generalisations for the *N*-particle 'cluster' problem, which has also been of long-standing interest. Here we consider approximations for the *N*-particle statistics directly based on Gaussian statistics, $P_N = G_N$, at least for the topological 'shape' of the cluster. The expressions for the joint probability density for purely Gaussian clusters can be obtained exactly as a function of the one- and two-particle dispersion, σ_1^2 and σ_r^2, but it is not listed here because of the lack of space.

Example: Line Source 'Plume' Results

For a definite example, consider an instantaneous line source (which approximates a point-source continuous plume in a mean wind). The *N*-th moment of absolute concentration along the centreline is

$$\overline{C^N} = (1-\rho)^{1-N}(1+(N-1)\rho)^{-1}\overline{C}^N \quad , \qquad (4)$$

where the mean concentration is $\overline{C} = (2\pi\sigma_1^2)^{-1}$ and both the one-particle dispersion, σ_1^2, and the two-particle displacement correlation coefficient, $\rho = \rho_2$, are functions of time which must be provided (see below).

From (4) we can exactly infer the scalar probability density function, but simply by comparison we remarkably recover Gifford's (1959) meandering plume result exactly. It is important to realise that the basis for this derivation is entirely different and does not explicitly rely on partitioning into separate meandering and plume-mixing dynamics. Other simple source geometries can be examined, but we only consider the plume result here. For the continuous point source in a mean wind the pdf for *scaled* concentration ϑ, along the centreline, is

$$P(\vartheta) = \varphi\vartheta^{\varphi-1}, \quad 0 \le \vartheta \le 1, \quad \varphi = 1/\rho - 1, \quad \vartheta = (1-\rho)C.$$

Two aspects are of note: first, the finite range of concentrations, and second, the collapse of the pdf far downstream when $\rho \sim 0$ i.e. $\varphi \sim \infty$. The latter means that the fluctuations of concentration vanish in the plume so that the instantaneous concentration is the same as the mean. This is not usually observed. The finite range of possible concentrations is not critical near the source with the maximum concentration unbounded like $(1-\rho)^{-1}$ as $\rho \sim 1$. Because we deal with infinite-peak initial sources we expect some large concentrations to persist, however the strong mixing caused by Gaussian statistics, represented in particular by too few small-separation displacements, causes rapid small-scale mixing grossly diluting all parcels of the plume. Clearly, non-Gaussian relative dispersion is important, both to generate plumes with realistic internal fluctuations and to model realistic peak concentrations. Incorporating such effects is particularly simple in our framework and is done by taking a 'sum' of Gaussian *N*-particle pdfs (G_N), weighted so that the relative dispersion pdf is exactly prescribed. Then at least the one-particle and two-particle information is correct within this framework.

Integral Transform for Non-Gaussian Effects

Suppose that $P_N = \int w(\rho) G_N d\rho$ for some $w \ge 0$, such that for the separation pdf $\wp(\underline{r})$, we have

$$\wp(\underline{r}) = \int_0^1 \frac{w(\rho)}{\left(4\pi\sigma_1^2(1-\rho)\right)^{3/2}} \exp\left(-\frac{r^2}{4(1-\rho)\sigma_1^2}\right) d\rho \; ; \qquad (5)$$

because of the linearity of (1) we also directly have

$$P(C) = \int_0^1 w(\rho) P(C;\rho) d\rho = \int_{\rho_{\min}}^1 w(\rho)/\rho\,(1-\rho)^{\varphi} C^{\varphi-1} d\rho \, ,$$

where $\rho_{\min} = 0$ for $C \le 1$ and $\rho_{\min} = 1 - C^{-2}$ for $C \ge 1$. Note that this pdf has no fixed maximum concentration unless $w(\rho)$ vanishes for $\rho \sim 1$, i.e. there is some weight for dispersion that remains highly correlated with patches of fluid with weak local dilution. In order to close the model we only require relative dispersion statistics (we are assuming that one-particle statistics are Gaussian and that the one-particle dispersion is known).

INERTIAL RANGE RESULTS

The key property is the separation pdf, $\wp(\underline{r})$ (obtained from $P_2(\underline{x}_1, \underline{x}_2)$) for which a useful parameterisation is

$$\wp(\underline{r}) = \gamma\left(1 - \tfrac{9}{8} C_\theta r^{2/3} \overline{\varepsilon}^{-1/3} t^{-1} + \lambda_2 r\right) e^{-\lambda_1 r - \frac{1}{4} r^2/\sigma_1^2} \qquad (6)$$

where the parameters are known by definition,

$$\lambda_1 = \lambda\sigma_r, \; \lambda_2 = \sigma_r, \; \gamma = \gamma(\lambda, \sigma_r), \; \lambda = \lambda(\alpha_{Ri}).$$

This form stresses the inertial subrange (Thomson, 1996) where (with velocity fluctuation σ_u), as an example,

$$\sigma_r^2 = \overline{r^2} \sim \alpha_{Ri} \overline{\varepsilon} t^3 << L^2 = \sigma_u^2 T^2 \qquad (7)$$

is the law for the growth of separation between pairs of particles. The Richardson constant α_{Ri} is widely thought to be quite small (α_{Ri} ~0.1 Elliot & Madja, 1996). The inertial range is important because it represents universal characteristics of turbulent flows and so has wider generic applicability. The dispersion inertial range is characterised by short-time mixing, with the one-particle dispersion approximated by $\sigma_1^2 \sim \sigma_u^2 t^2 \ll L^2$, but can last for significant periods of time (up to 15 minutes) in typical turbulence in the convective boundary layer of the atmosphere, at least for plumes far enough away from the surface layer. Later we relax small-time restrictions.

Form (6) ensures Corrsin-Obukhov similarity for scalar fields (Monin & Yaglom, 1975) and is intrinsically non-Gaussian. In principle, (6) can be obtained from two-particle Lagrangian stochastic modelling (Borgas & Sawford, 1996; Franzese & Borgas, 1998), but no model has yet been devised to properly include inertial-range effects, i.e. with reasonable values of $C_\theta \sim 3.2$. The correlation coefficient for two-particle displacements,

$$\rho_2 = 1 - \sigma_r^2 / 6\sigma_1^2 = 1 - \alpha_{Ri}\, \bar{\varepsilon} t / 6\sigma_u^2 \sim 1 \quad (t \ll T),$$

becomes a surrogate for time in our work. We use (6) in (5) (inverted) to test the role of non-Gaussian effects. The centreline concentration pdf is shown in figure 5 for the

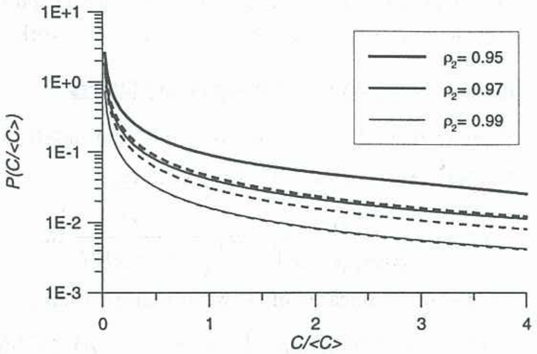

Figure 5 : Concentration probability density function near the source: dashed lines are Gifford's results.

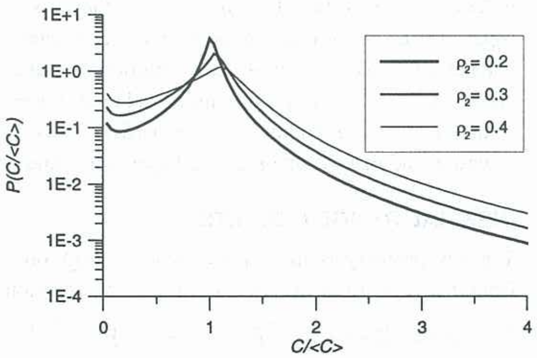

Figure 6 : Concentration probability density function far downstream. A peak develops at the mean concentration.

three times corresponding to $\rho_2 = 0.99, 0.97, 0.95$, i.e. near source when pair motions are highly correlated (but for atmospheric flows well beyond any viscous zone). Gifford's results are shown as dashed curves. It is clear that the quantitative differences grow slowly with time, with the later times considered here perhaps beyond inertial-range scaling times. Qualitatively there is almost no difference. To examine more dramatic behaviour we now consider much further downstream when ρ_2 is smaller (0.2, 0.3 0.4) as shown in figure 6. These results still use (6), but with effective modifications of the Corrsin-Obukhov $r^{2/3}$-law coefficient to the form $3/8 C_\theta r^{2/3} \bar{\varepsilon}^{-1/3} t^{-1}$, which accounts for the dominant single-particle diffusion-like dispersion far downstream in contrast to (7). These results show that for this model, while a strong peak may develop near the mean concentration, more complex bimodal behaviour is possible with a peak at zero concentration (intermittency) and a long tail towards infinite concentrations.

CONCLUSION

A new interpretation of a passive scalar plume in turbulent flow is given, updating Gifford's (1959) original meandering plume. A multi-particle Lagrangian framework exploits near Gaussian-like behaviour for the shape of multi-particle clusters, tested here for new three-particle results. The size of a multi-particle cluster is essentially traditional relative dispersion, which is much studied. Scalar probability densities along the centreline of a point source plume are determined for simple parameterised (but non-Gaussian) relative dispersion, but the method has scope for wider applications and reinforces the need to study relative dispersion in detail.

ACKNOWLEDGEMENTS

Thanks to Assoc. Professor P.K. Yeung of Georgia Institute of Technology, for his numerical data and advice (courtesy of NSF Grant INT-9526868 and DIST Bilateral Exchange 95/4358), and to Dr Brian Sawford of CSIRO Atmospheric Research, for much guidance.

REFERENCES

BORGAS, M.S. & SAWFORD, B.L., "Molecular diffusion and viscous effects in grid turbulence", *J. Fluid. Mech.* **324**:25-54, 1996.

ELLIOT F.W. & MADJA A.J., "Pair dispersion over an inertial range spanning many decades", *Phys. Fluids* **8**:1052-1060, 1996.

FRANZESE P.& BORGAS M.S., "A relative dispersion model for turbulent flow", *In preparation*. 1998.

GIFFORD, F.A., "Statistical properties of a fluctuating plume dispersion model", *Adv. Geophys.* **6**:117-137, 1959.

MONIN A.S. & YAGLOM A.M., *Statistical Fluid Mechanics*. Vol. II. Ed. J.L. Lumley, M.I.T. Press. Cambridge, MA, 1975.

SAWFORD B.L., "Lagrangian statistical simulation of concentration mean and fluctuating fields", *J. Climate Appl. Meteor.* **24**:1152-1166, 1985.

THOMSON, D.J., "The second-order moment structure of dispersing plumes and puffs", *J. Fluid. Mech.* **320**:305-329, 1996.

YEUNG, P.K., "Direct numerical simulation of two-particle relative diffusion in isotropic turbulence", *Phys. Fluids.* **6**:3416-3428, 1994.

YEUNG, P.K., private communication, 1997.